A

Publication	Type	DIV	Strain	Silencing	Timepoints
Calderon, et al. eLife (2022)	Cortical	10	CD-1	O/N D-AP5/TTX	1hr, 6hr
Ibarra, et al. Mol Sys Bio (2022)	Cortical	7	CD-1	2hr AP5/TTX	1hr, 6hr, 10hr
Maze, et al. Neuron (2015)	Cortical	8	C57BL/6	1hr D-AP5/TTX	30min, 2hr, 5hr
Xu, et al. Biology (2022)	Cortical	7	C57BL/6	O/N DL-AP5/TTX	2hr, 6hr
Quesnel-Valllieres, et al. Mol Cell (2016)	Hippocampal	10	C57BL/6	No silencing	30min, 3hr

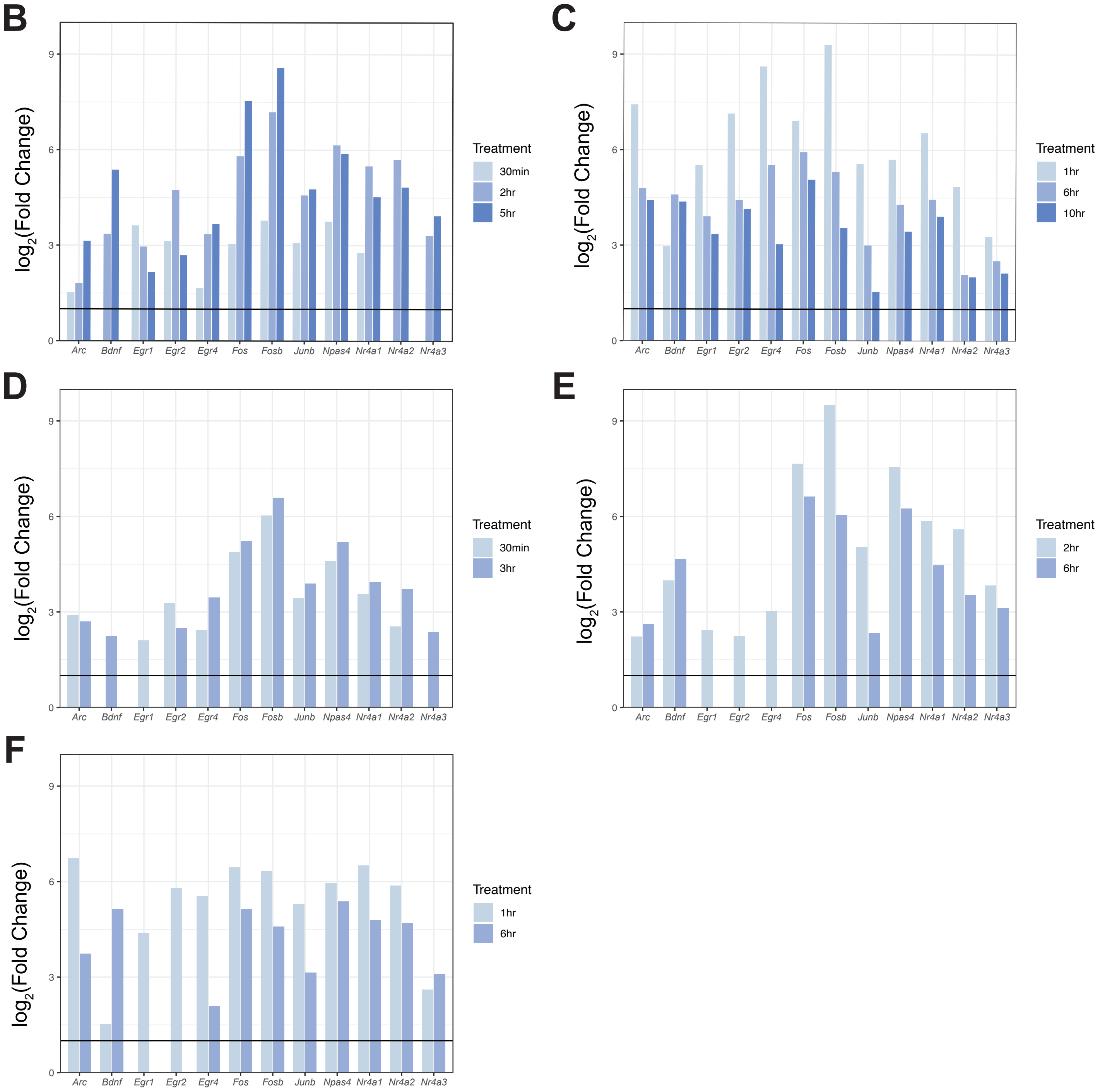

Supplemental Figure 1. Immediate early gene expression is triggered after KCl treatment in all datasets. (A) Table denoting the experimental parameters used to generate each dataset. (B-E) Log_2 fold change in expression of immediate early genes between KCl and control samples across all datasets included in the analysis; (B) Maze et al. 2015, (C) Ibarra et al. 2022, (D) Quesnel-Vallieres et al. 2016, (E) Xu et al. 2022, (F) Calderon et al. 2022. Dashed line denotes no change in expression ($\log_2 FC = 1$).

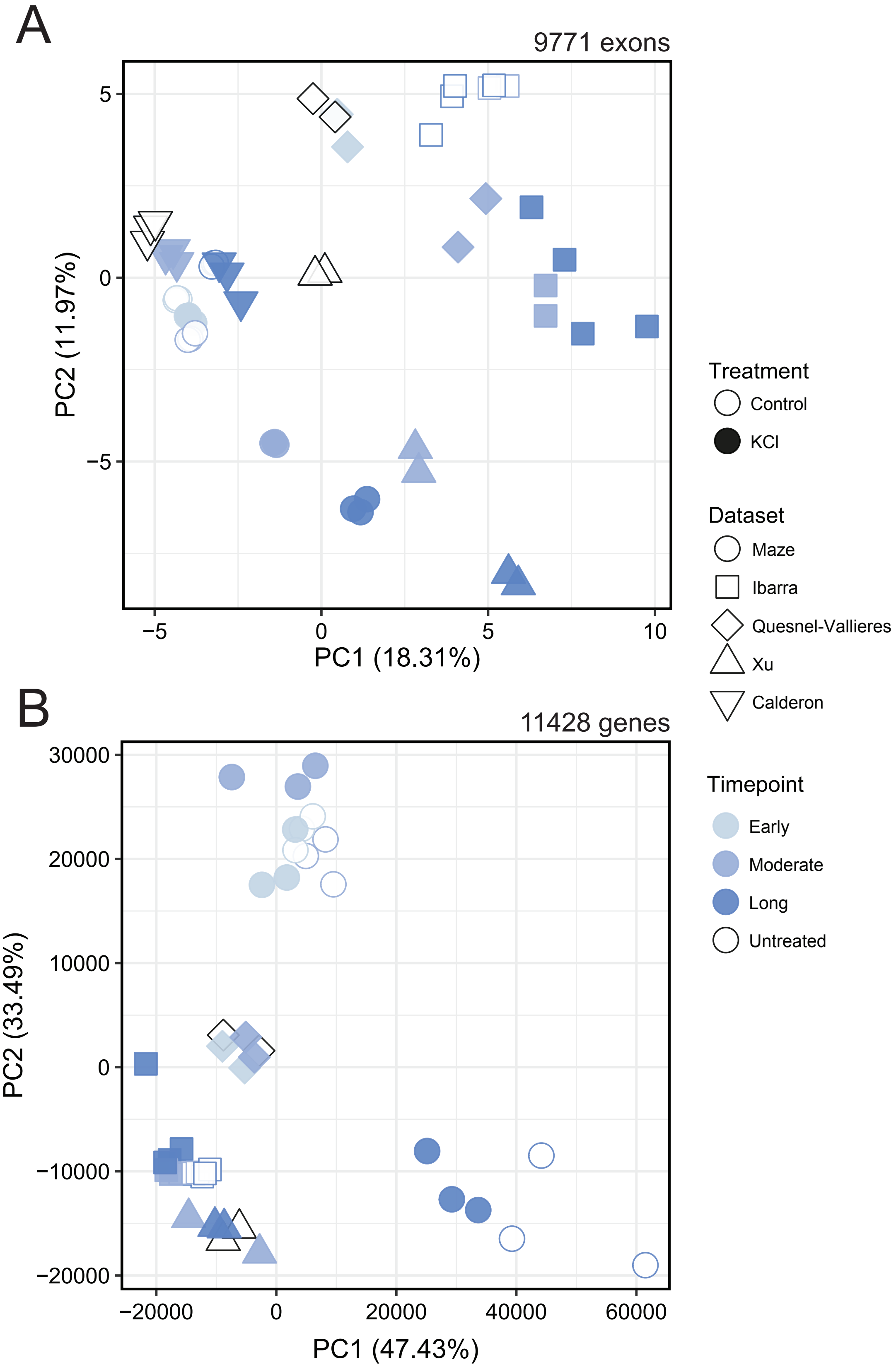
A
9771 exons
PC2 (11.97%)
PC1 (18.31%)
5
0
−5
−5
0
5
10
B
11428 genes
PC2 (33.49%)
PC1 (47.43%)
30000
20000
10000
0
−10000
−20000
−20000
0
20000
40000
60000
Treatment
Control
KCl
Dataset
Maze
Ibarra
Quesnel-Vallieres
Xu
Calderon
Timepoint
Early
Moderate
Long
Untreated

Supplemental Figure 2. KCl-stimulated samples across different datasets converge at the level of alternative splicing. (A) PCA of inclusion of 9,771 exons quantified in all datasets used in this work plotted within the same PCA space. Fill denotes KCl status, fill color represents time after stimulation, and shape denotes dataset of origin. Percent of variance each principal component represents is shown on each axis. (B) PCA of expression of 11,428 genes quantified in all datasets used in this work plotted within the same PCA space. Fill denotes KCl status, fill color represents time after stimulation, and shape denotes dataset of origin. Percent of variance each principal component represents is shown on each axis.

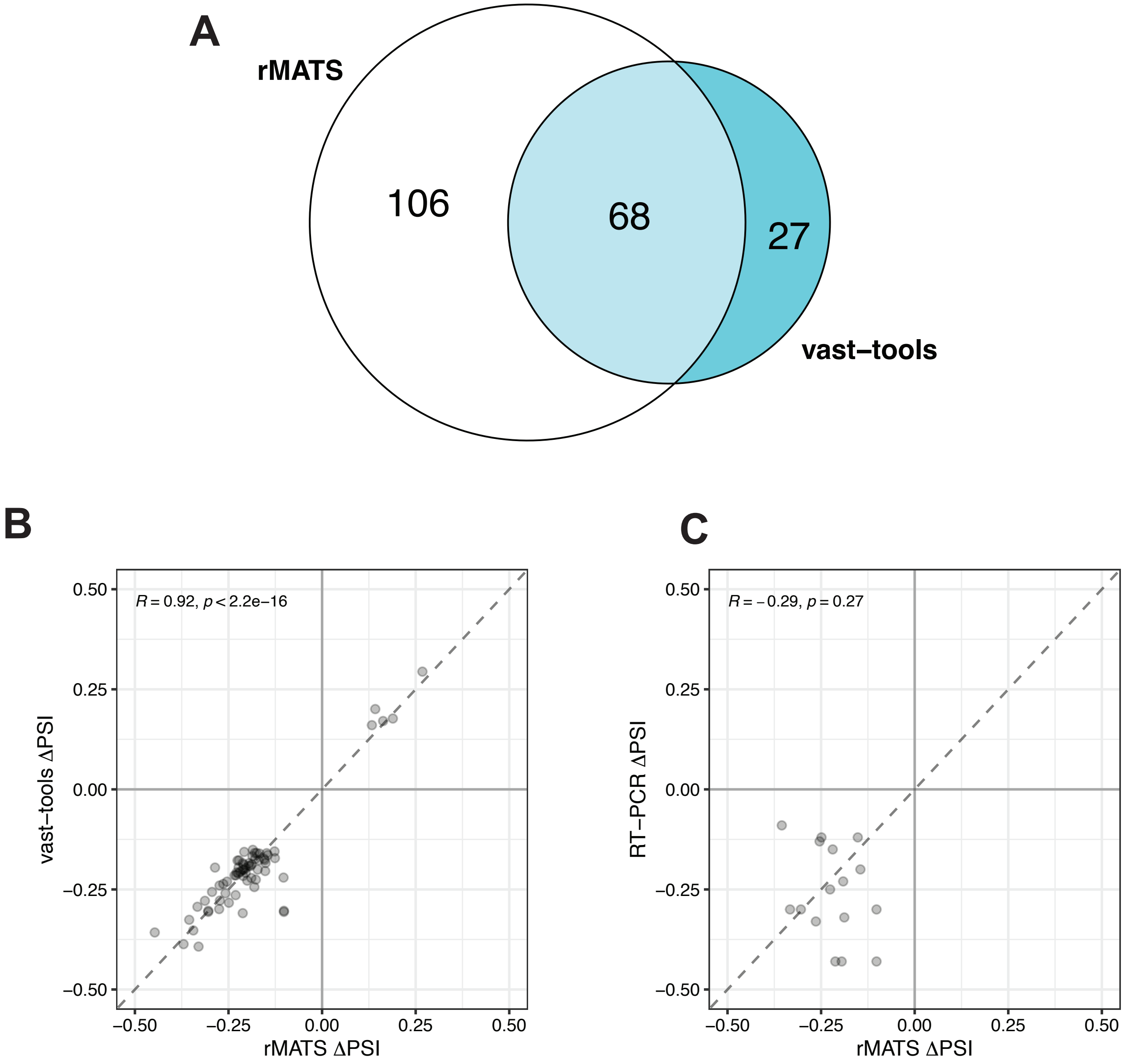
A
rMATS
106
68
27
vast−tools
B
R = 0.92, p < 2.2e−16
vast−tools ΔPSI
rMATS ΔPSI
0.50
0.25
0.00
−0.25
−0.50
−0.50
−0.25
0.00
0.25
0.50
C
R = −0.29, p = 0.27
RT−PCR ΔPSI
rMATS ΔPSI
0.50
0.25
0.00
−0.25
−0.50
−0.50
−0.25
0.00
0.25
0.50

Supplemental Figure 3. KCl-dependent microexons are identified by rMATS. (A) Euler plot showing the overlap of differentially spliced microexons (<28nt) after 3h of KCl treatment called by vast-tools in Quesnel-Vallieres et al. and rMATS in this study. (B) Scatterplot of microexon ∆PSIs called by vast-tools and rMATS. Correlation was calculated using Pearson’s R. (C) Scatterplot of ∆PSIs for KCl-dependent microexons called by rMATS and validated by reverse transcription PCR (RT-PCR) in Quesnel-Vallieres et al.

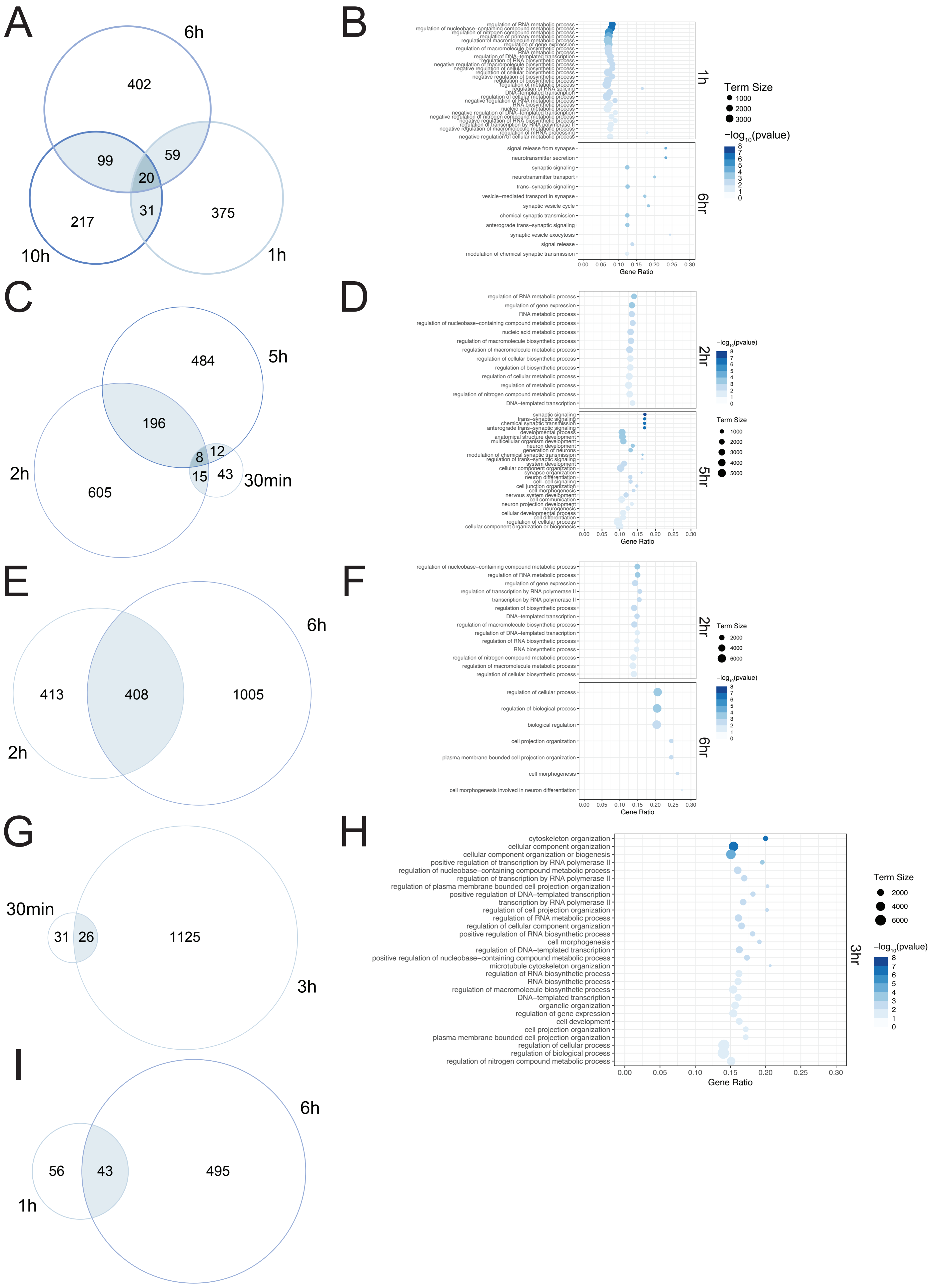
A
6h
402
99
59
20
217
31
375
10h
1h
B
regulation of RNA metabolic process
regulation of nucleobase–containing compound metabolic process
regulation of nitrogen compound metabolic process
regulation of primary metabolic process
regulation of macromolecule metabolic process
regulation of gene expression
regulation of macromolecule biosynthetic process
RNA metabolic process
regulation of DNA–templated transcription
regulation of RNA biosynthetic process
negative regulation of macromolecule biosynthetic process
negative regulation of cellular biosynthetic process
regulation of cellular biosynthetic process
negative regulation of biosynthetic process
regulation of biosynthetic process
regulation of metabolic process
regulation of RNA splicing
DNA–templated transcription
regulation of cellular metabolic process
negative regulation of RNA metabolic process
RNA biosynthetic process
nucleic acid metabolic process
negative regulation of DNA–templated transcription
negative regulation of nitrogen compound metabolic process
negative regulation of RNA biosynthetic process
regulation of transcription by RNA polymerase II
negative regulation of macromolecule metabolic process
regulation of mRNA processing
negative regulation of cellular metabolic process
1h
signal release from synapse
neurotransmitter secretion
synaptic signaling
neurotransmitter transport
trans–synaptic signaling
vesicle–mediated transport in synapse
synaptic vesicle cycle
chemical synaptic transmission
anterograde trans–synaptic signaling
synaptic vesicle exocytosis
signal release
modulation of chemical synaptic transmission
6hr
0.00 0.05 0.10 0.15 0.20 0.25 0.30
Gene Ratio
Term Size
1000
2000
3000
$-\log_{10}$(pvalue)
8 7 6 5 4 3 2 1 0
C
484
5h
196
2h
8
12
15
43
30min
605
D
regulation of RNA metabolic process
regulation of gene expression
RNA metabolic process
regulation of nucleobase–containing compound metabolic process
nucleic acid metabolic process
regulation of macromolecule biosynthetic process
regulation of macromolecule metabolic process
regulation of cellular biosynthetic process
regulation of biosynthetic process
regulation of cellular metabolic process
regulation of metabolic process
regulation of nitrogen compound metabolic process
DNA–templated transcription
2hr
$-\log_{10}$(pvalue)
8 7 6 5 4 3 2 1 0
synaptic signaling
trans–synaptic signaling
chemical synaptic transmission
anterograde trans–synaptic signaling
developmental process
anatomical structure development
multicellular organism development
neuron development
generation of neurons
modulation of chemical synaptic transmission
regulation of trans–synaptic signaling
system development
cellular component organization
synapse organization
neuron differentiation
cell–cell signaling
cell junction organization
cell morphogenesis
nervous system development
cell communication
neuron projection development
neurogenesis
cellular developmental process
cell differentiation
regulation of cellular process
cellular component organization or biogenesis
5hr
Term Size
1000
2000
3000
4000
5000
0.00 0.05 0.10 0.15 0.20 0.25 0.30
Gene Ratio
E
6h
413
408
1005
2h
F
regulation of nucleobase–containing compound metabolic process
regulation of RNA metabolic process
regulation of gene expression
regulation of transcription by RNA polymerase II
transcription by RNA polymerase II
regulation of biosynthetic process
DNA–templated transcription
regulation of macromolecule biosynthetic process
regulation of DNA–templated transcription
regulation of RNA biosynthetic process
RNA biosynthetic process
regulation of nitrogen compound metabolic process
regulation of macromolecule metabolic process
regulation of cellular biosynthetic process
2hr
Term Size
2000
4000
6000
$-\log_{10}$(pvalue)
8 7 6 5 4 3 2 1 0
regulation of cellular process
regulation of biological process
biological regulation
cell projection organization
plasma membrane bounded cell projection organization
cell morphogenesis
cell morphogenesis involved in neuron differentiation
6hr
0.00 0.05 0.10 0.15 0.20 0.25 0.30
Gene Ratio
G
30min
31
26
1125
3h
H
cytoskeleton organization
cellular component organization
cellular component organization or biogenesis
positive regulation of transcription by RNA polymerase II
regulation of nucleobase–containing compound metabolic process
regulation of transcription by RNA polymerase II
regulation of plasma membrane bounded cell projection organization
positive regulation of DNA–templated transcription
transcription by RNA polymerase II
regulation of cell projection organization
regulation of RNA metabolic process
regulation of cellular component organization
positive regulation of RNA biosynthetic process
cell morphogenesis
regulation of DNA–templated transcription
positive regulation of nucleobase–containing compound metabolic process
microtubule cytoskeleton organization
regulation of RNA biosynthetic process
RNA biosynthetic process
regulation of macromolecule biosynthetic process
DNA–templated transcription
organelle organization
regulation of gene expression
cell development
cell projection organization
plasma membrane bounded cell projection organization
regulation of cellular process
regulation of biological process
regulation of nitrogen compound metabolic process
3hr
Term Size
2000
4000
6000
$-\log_{10}$(pvalue)
8 7 6 5 4 3 2 1 0
0.00 0.05 0.10 0.15 0.20 0.25 0.30
Gene Ratio
I
6h
56
43
495
1h

Supplemental Figure 4. Different lengths of KCl stimulation induce distinct alternative splicing patterns. (A) Euler plot of differentially spliced exons across KCl timepoints from Ibarra, et al. (B) Enriched Gene Ontology terms for each KCl timepoint from Ibarra, et al. All significant terms from the “Biological Process” set are shown. Timepoints which returned no significantly enriched terms are not shown. (C) Euler plot of differentially spliced exons across KCl timepoints from Maze, et al. (D) Enriched Gene Ontology terms for each KCl timepoint from Maze, et al. All significant terms from the “Biological Process” set are shown. Timepoints which returned no significantly enriched terms are not shown. (E) Euler plot of differentially spliced exons across KCl timepoints from Xu, et al. (F) Enriched Gene Ontology terms for each KCl timepoint from Xu, et al. All significant terms from the “Biological Process” set are shown. Timepoints which returned no significantly enriched terms are not shown. (G) Euler plot of differentially spliced exons across KCl timepoints from Quesnel-Vallieres, et al. (H) Enriched Gene Ontology terms for each KCl timepoint from Quesnel-Vallieres, et al. All significant terms from the “Biological Process” set are shown. Timepoints which returned no significantly enriched terms are not shown. (I) Euler plot of differentially spliced exons across KCl timepoints from Calderon, et al. Note, no enriched Gene Ontology terms were found for either timepoint.

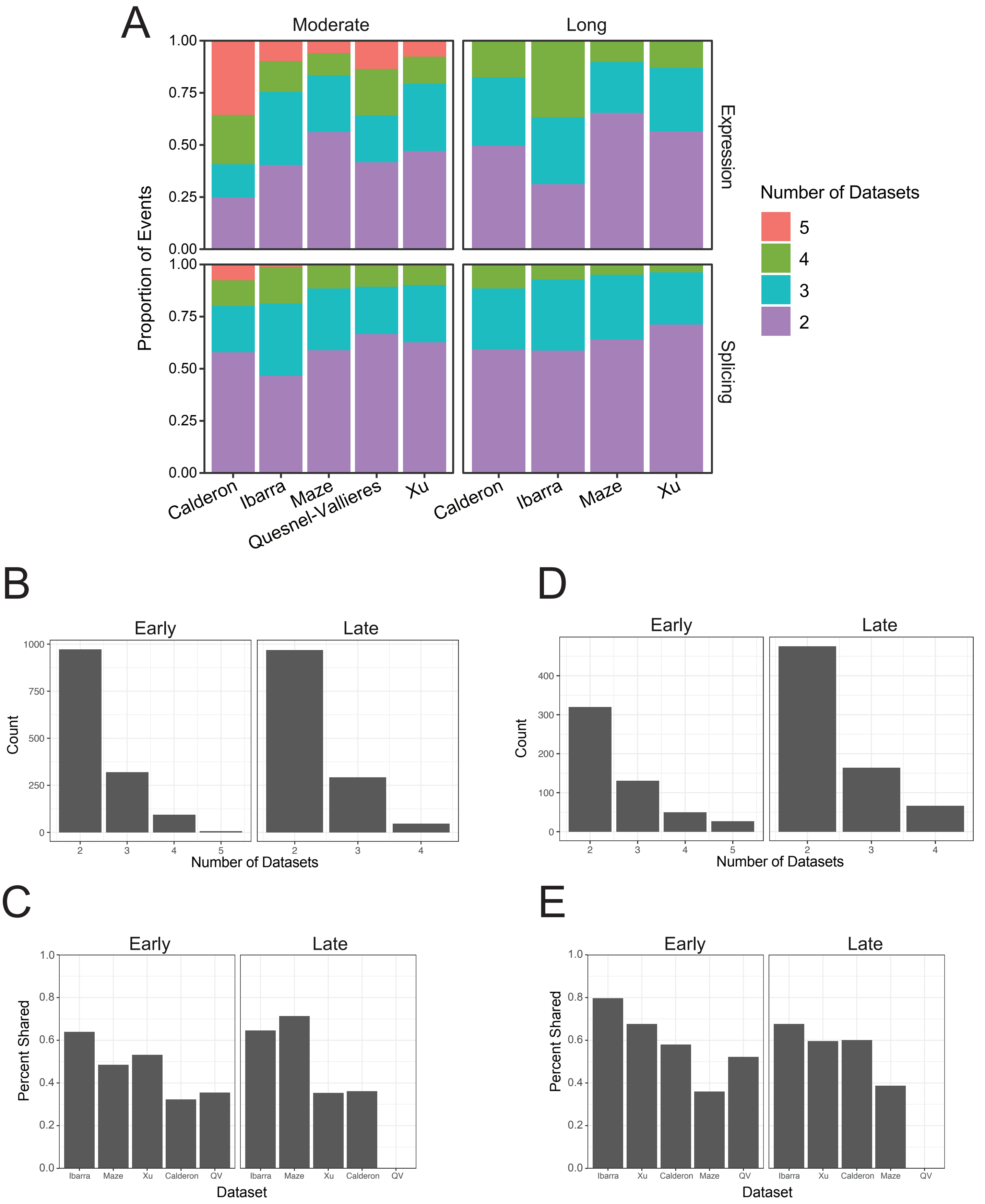
A
Moderate
Long
Expression
Splicing
Proportion of Events
1.00
0.75
0.50
0.25
0.00
Calderon
Ibarra
Maze
Quesnel-Vallieres
Xu
Number of Datasets
5
4
3
2
B
Early
Late
Count
1000
750
500
250
0
2
3
4
5
Number of Datasets
C
Percent Shared
1.0
0.8
0.6
0.4
0.2
0.0
Ibarra
Maze
Xu
Calderon
QV
Dataset
D
400
300
200
100
E

Supplemental Figure 5. KCl-dependent differentially spliced exons and differentially expressed genes are consistent across datasets. (A) Number of datasets which share a differential alternative exon or DEG found in each dataset. (B) Number of datasets in which a given high-confidence KCl-dependent exon is found. (C) Proportion of each dataset in which a differential alternative exon is found in another dataset. (D) Number of datasets in which a given high-confidence KCl-dependent DEG is found. (E) Proportion of each dataset in which a DEG is found in another dataset.

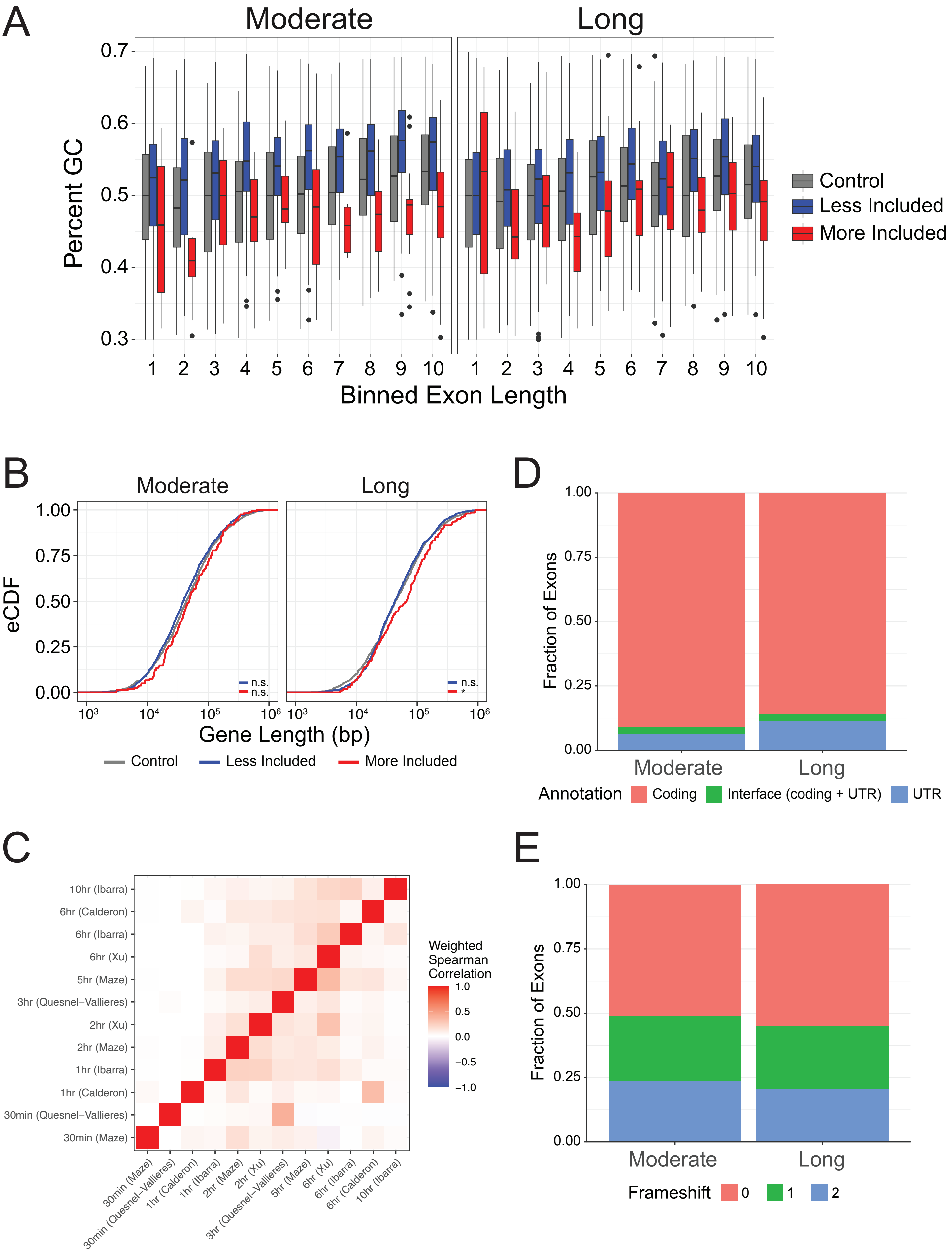
A
Moderate
Long
Percent GC
0.7
0.6
0.5
0.4
0.3
1 2 3 4 5 6 7 8 9 10
Binned Exon Length
Control
Less Included
More Included
B
Moderate
Long
eCDF
1.00
0.75
0.50
0.25
0.00
n.s.
n.s.
n.s.
*
10^3 10^4 10^5 10^6
Gene Length (bp)
Control
Less Included
More Included
C
10hr (Ibarra)
6hr (Calderon)
6hr (Ibarra)
6hr (Xu)
5hr (Maze)
3hr (Quesnel−Vallieres)
2hr (Xu)
2hr (Maze)
1hr (Ibarra)
1hr (Calderon)
30min (Quesnel−Vallieres)
30min (Maze)
Weighted Spearman Correlation
1.0
0.5
0.0
−0.5
−1.0
D
Fraction of Exons
1.00
0.75
0.50
0.25
0.00
Moderate
Long
Annotation
Coding
Interface (coding + UTR)
UTR
E
Fraction of Exons
1.00
0.75
0.50
0.25
0.00
Moderate
Long
Frameshift
0
1
2

Supplemental Figure 6. KCl-dependent exons are marked by particular features. (A) Cumulative distribution function across total gene length for KCl-dependent (blue and red lines) and control exons (grey line). (B) Percent GC across exon length bins. Each bin contains an equal number of exons for each group. (C) Heatmap of weighted Spearman Rank correlations between all datasets used in analysis (see Methods for description of calculation). Datasets categorized as “moderate” and “long” after KCl stimulation are designated. Q-V is equivalent to Quesnel-Vallieres, et al. (D) Fraction of KCl-dependent exons classified as translated and untranslated. Annotations are taken from GENCODE annotations of mm39 (v31). (E) Fraction of KCl-dependent exons exhibiting a 0, +1, or +2 frameshift. Frameshifts are calculated based on exon length being a multiple of three.

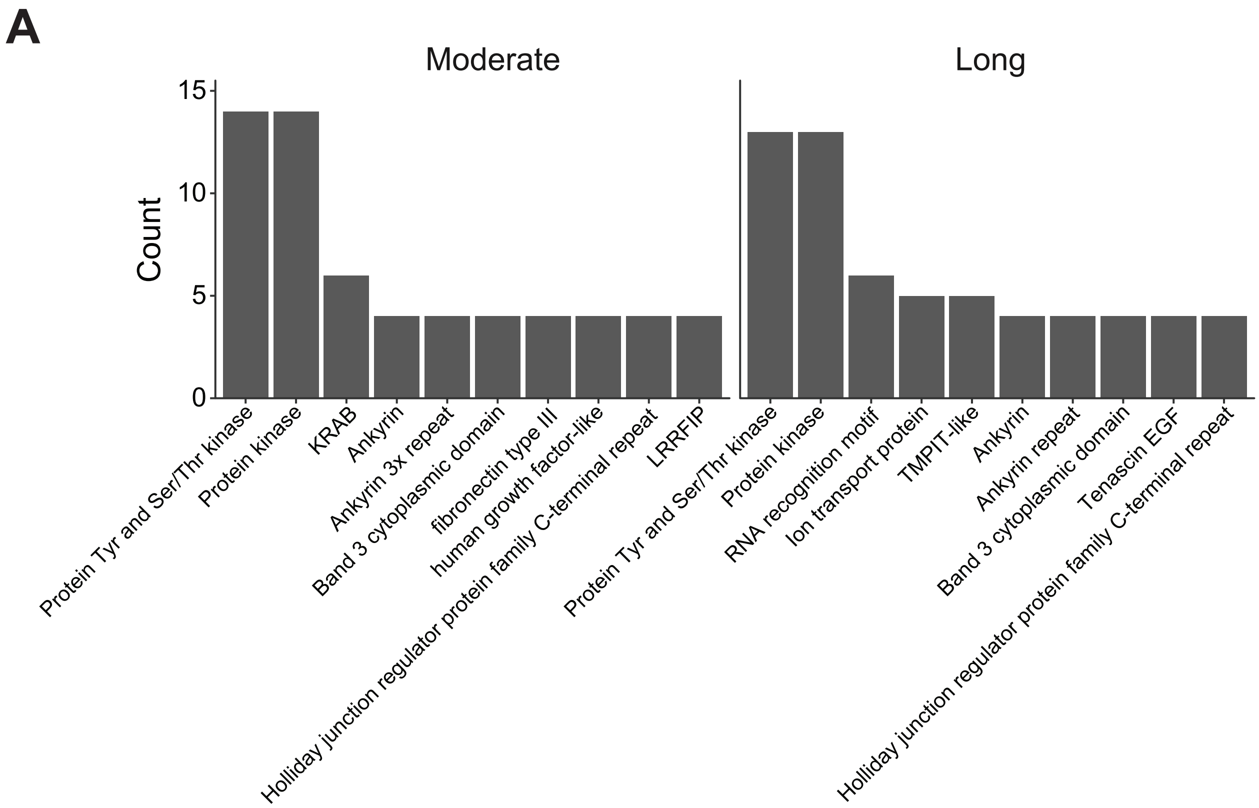
A
Moderate
Long
Count
0
5
10
15
Protein Tyr and Ser/Thr kinase
Protein kinase
KRAB
Ankyrin
Ankyrin 3x repeat
Band 3 cytoplasmic domain
fibronectin type III
human growth factor-like
Holliday junction regulator protein family C-terminal repeat
LRRFIP
Protein Tyr and Ser/Thr kinase
Protein kinase
RNA recognition motif
Ion transport protein
TMPIT-like
Ankyrin
Ankyrin repeat
Band 3 cytoplasmic domain
Tenascin EGF
Holliday junction regulator protein family C-terminal repeat

Supplemental Figure 7. High confidence KCl-dependent exons alter the coding potential of a diverse group of functional protein domains. (A) left, top 10 most frequently overlapping Pfam domains with moderate high confidence KCl-dependent exons that do not induce a frameshift; right, top 10 most frequently overlapping Pfam domains with long high confidence KCl-dependent that do not induce a frameshift.

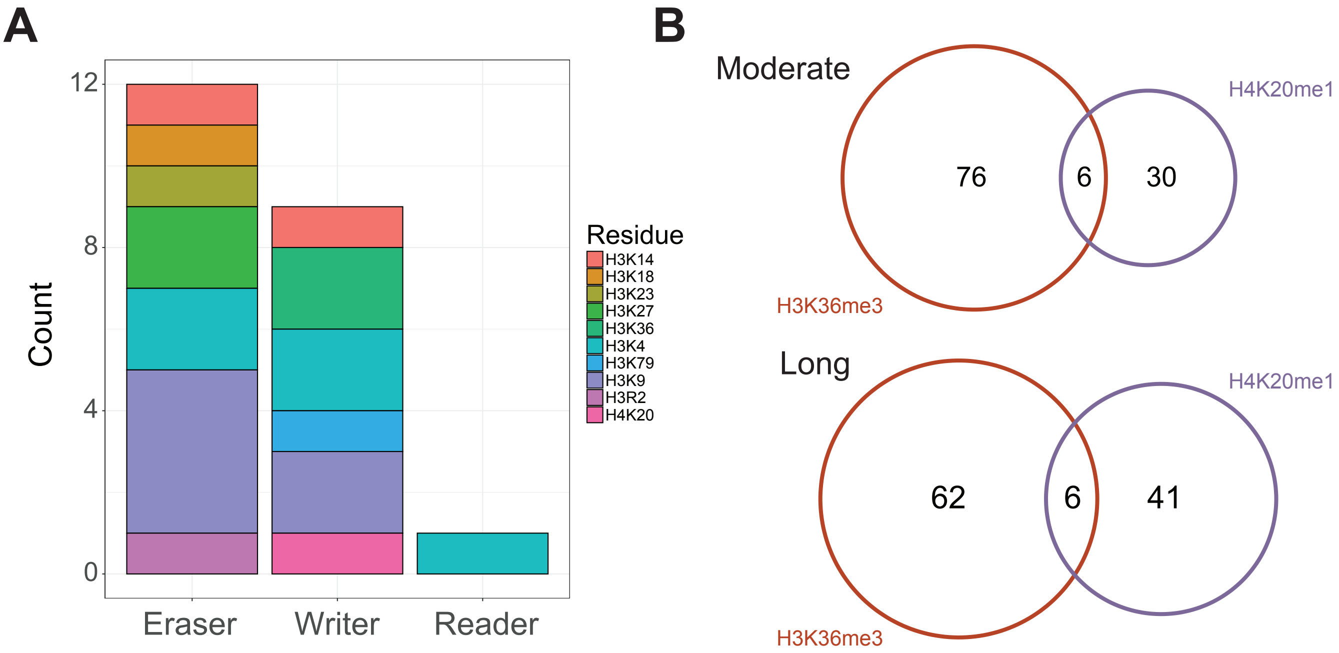
A
Count
12
8
4
0
Eraser
Writer
Reader
Residue
H3K14
H3K18
H3K23
H3K27
H3K36
H3K4
H3K79
H3K9
H3R2
H4K20
B
Moderate
H4K20me1
76
6
30
H3K36me3
Long
H4K20me1
62
6
41
H3K36me3

Supplemental Figure 8. KCl treatment alters the splicing of many histone modifying enzymes. (A) Stacked bar graph of genes under the GO term “histone modification” whose splicing is altered by KCl. Color denotes the primary target residue. (B) Euler plot of KCl-dependent exons under KCl-dependent H3K36me3 or H4K20me1 peaks.

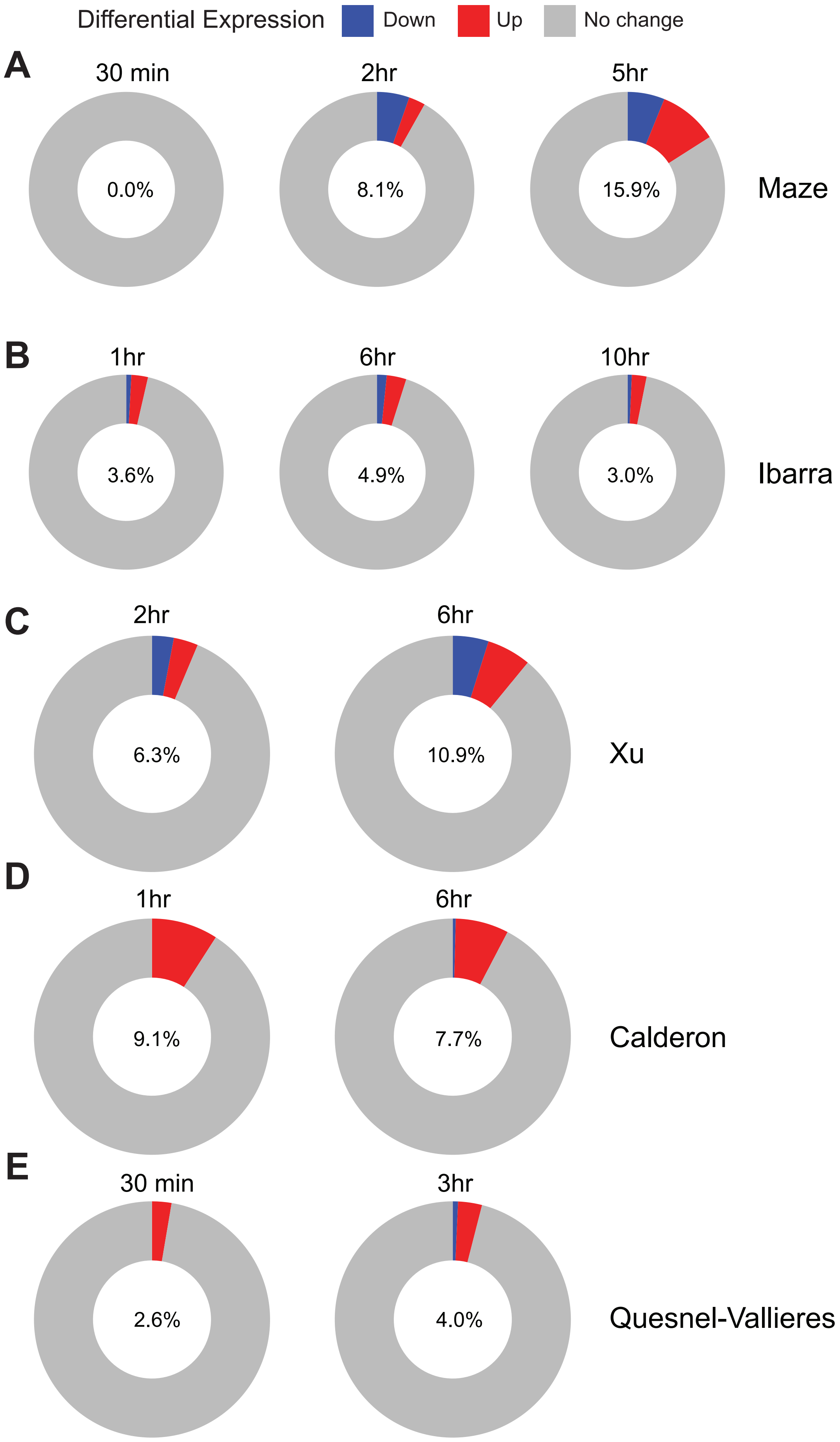
Differential Expression
Down
Up
No change
A
30 min
0.0%
2hr
8.1%
5hr
15.9%
Maze
B
1hr
3.6%
6hr
4.9%
10hr
3.0%
Ibarra
C
2hr
6.3%
6hr
10.9%
Xu
D
1hr
9.1%
6hr
7.7%
Calderon
E
30 min
2.6%
3hr
4.0%
Quesnel-Vallieres

Supplemental Figure 9. Genes containing frameshifted, KCl-dependent exons are not differentially expressed. (A) Proportion of frameshifting, KCl-dependent exons which are also differentially expressed in Maze, et al. using relaxed cutoffs ($L2FC > 1$; $p.adj < 0.05$). Percentage at the center of each plot denotes the percentage of exons which are differentially expressed (both up- and down-regulated). (B) Same as (A) for Ibarra, et al. (C) Same as (A) for Xu, et al. (D) Same as (A) for Calderon, et al. (E) Same as (A) Quesnel-Vallieres, et al.